Earthquake Engineering, Tenth World Conference © 1992 Balkema, Rotterdam. ISBN 90 5410 060 5

Seismic analysis of frames with viscoelastic beam-column connections

S.Y. Hsu & A. Fafitis
Civil Engineering Department, Arizona State University, Ariz., USA

ABSTRACT: A new viscoelastic-type isolation connection (damper) consisting of two steel plates interlocked by single tooth and elastomeric material was developed and tested recently at the Earthquake Laboratory of Arizona State University. Based on experimental results, a Kelvin-Voigt type model was developed to simulated the behavior of this isolator. Comparisons of stress-strain curves obtained from the model and from tests indicate that the model describes the behavior of the device with acceptable accuracy. A numerical method has been developed to analyze the response of framed structures equipped with these new viscoelastic-type connections. The effectiveness of the device is studied numerically and comparison of the response of isolated structures to earthquake excitation indicated greatly improved behavior.

1 INTRODUCTION

The concept of using an isolation device to protect a structure from earthquake disturbances has been used in two different forms, base isolation and connection isolation. The base isolator is designed to isolate the structure at its base from intense earthquake motion to contain the relative displacement between the structure and the foundation in an acceptable range. A variety of designs for base isolation systems, including laminated rubber bearing, roller bearing, and friction type, have been developed (Kelly 1982, Mostaghel and Khodaverdian 1987, Kelly and Koh 1990, Ahmadi et al. 1990).

The connection isolation is aimed at dissipating the earthquake energy by placing the isolation device at selected connections of the structure. Among the best known are the friction-type and the viscoelastic-type. The viscoelastic-type isolation systems are the commonly used. They are usually made of alternating layers of elastomeric material and steel. A number of structures with added viscoelastic damper have been investigated (Mahmoodi 1969, 1974, Gasparini et al. 1980, 1981, Bergman and Hanson 1986, Zhang et al. 1989). It has been shown that the incorporating of these isolation devices into structures, especially for high rise buildings, is beneficial and improves the response to wind as well as earthquake excitation (Mahmoodi and Keel 1986, Lin et al. 1991).

A new type of isolation connection consisting of two steel plates interlocked by a single tooth and elastomeric material was developed and tested in the Earthquake Laboratory of the Civil Engineering Department of the Arizona State University. The profile of this single-tooth isolation connection is shown in Fig. 1. Based on these experimental data, a Kelvin-Voigt type model was developed to simulate the behavior of the connection. A structural model has been developed for the analysis of structures equipped with this type of isolation device. In this study, three different numerical earthquake records were used as input ground motions, and the non-linear time-history dynamic analysis of two unbraced frames were used to study the seismic response of the proposed structural system. The results of the dynamic analysis of structures with isolation connections and the computed response of identical structures with conventional connections, were used to investigate the effectiveness of the isolation system.

2 CONNECTION MODEL

A Kelvin-Voigt type model consisting of a spring and dashpot in parallel was used to simulate the behavior of the proposed single-tooth connection isolation shown in Fig. 1. The derivation of the equations of the model is given elsewhere (Hsu and Fafitis 1990, Hsu and Fafitis 1992b). The stress-strain relationship is expressed as follows

$$\sigma_i = \frac{\eta_i (\varepsilon_{i+1} - \varepsilon_i)}{(t_{i+1} - t_i)} + E\varepsilon_i \qquad (1)$$

where E is the estimated elastic modulus given by the empirical formula

$$E = -44.504 + 2.44D - 0.0392D^2 + 0.00021D^3 \qquad (2)$$

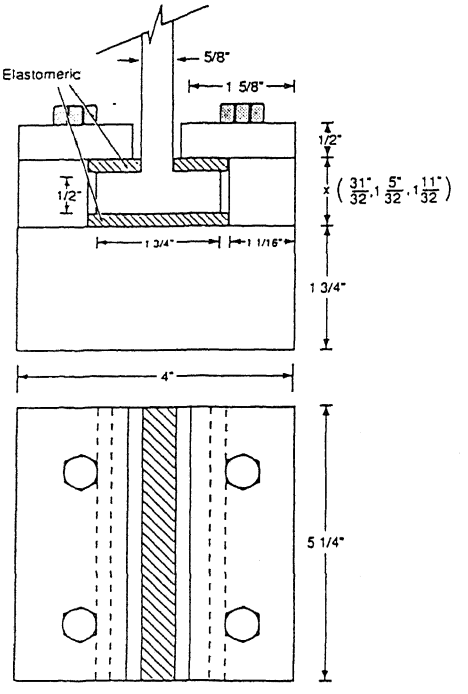

Fig. 1. Profile of single-tooth connection.

where E is in Ksi, and D is the durometer, the measure of the hardness of elastomeric material. The durometer is scaled from 0 (soft) to 100 (hard). In this study, durometers from 40 to 95 were used.

In eq. (1), the viscosity coefficient h_i is expressed as

$$\eta_i = A\,\varepsilon_i \tag{3}$$

where A is the viscosity factor in Ksi-sec. For frequencies between 0.5 Hz and 1.5 Hz, which are of interest in earthquake design, the viscosity factor A can be expressed as follows:

For loading,

$$A = 5.837-0.284D+0.00463D^2-0.0000218D^3 \tag{4}$$

for unloading,

$$A = -29.203+1.592D-0.0255D^2+0.000137D^3 \tag{5}$$

Because of the unsymmetrical configuration of the device, the elastic modulus and the viscosity factor for tension can be calculated by the following formulas

$$E_c = S\,E_t \tag{6}$$

$$A_c = S^2\,A_t \tag{7}$$

where E_C, E_t, A_C and A_t are the elastic moduli and viscosity factors for compression and tension, respectively. S is a shape constant which for the configuration studied in this research can be taken as 1.9.

3 STRUCTURAL MODEL

The configuration of the dissipative connection is shown in Fig. 2. The energy dissipating device described earlier is attached symmetrically to the top and bottom flange of the beam and to the column. The shear is transferred through a shear pin connection. Thus, the energy dissipating device is subjected only to axial forces provided that the rotations of the hinge are small. The above connection is modeled as shown in Fig. 3. where the elastic rheological properties of the beam element are modeled by the twisting spring and dashpot. This modeling is consistent with the traditional assumption of plastic hinge.

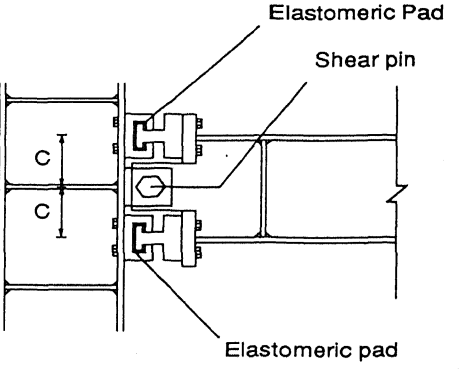

Fig. 2. Beam-column connection with single-tooth connection.

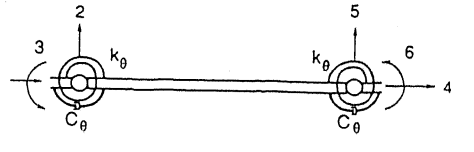

Fig. 3.Modeling of beam element with single-tooth connection.

In order to establish the moment-rotation relationship of the connection, the following assumptions are made: (1) the stresses are uniformly distributed over the elastomeric material, and the stress at the center of the elastomeric material is taken as the magnitude of this uniform stress, and (2) the joint rotation angle, θ, is assumed to be small. The equilibrium equation of the moment, M, about the center of the hinge is expressed as

$$M = \sigma_c a_c C + \sigma_t a_t C \tag{8}$$

where a_c and a_t are the areas of elastomeric material in compression and tension. σ_c and σ_t are the compression and tension stresses of elastomeric material, and C is the distance from the center of the hinge to the center line of each of the two devices as shown in Fig. 2. Note that the compression in each of the two devices is defined as the axial force causing compression of the large (bottom) pad of Fig. 1, and the tension is defined as the axial force causing the compression of the top pad.

Substituting eq. (1) into eq. (8) gives

$$M = (E_c\varepsilon_c+\eta_c\dot{\varepsilon}_c)a_c C + (E_t\varepsilon_t+\eta_t\dot{\varepsilon}_t)a_t C \tag{9}$$

substituting eq. (3) into eq. (9) gives

$$M = \left[E_c \frac{C\theta}{h_c} + (A_c \frac{C\theta}{h_c})\frac{C\dot{\theta}}{h_c} \right] a_c C + \left[E_t \frac{C\theta}{h_t} + (A_t \frac{C\theta}{h_t})\frac{C\dot{\theta}}{h_t} \right] a_t C$$

$$= \left[(\frac{E_c a_c}{h_c} + \frac{E_t a_t}{h_t}) C^2 \right] \theta + \left[(\frac{A_c a_c}{h_c^2} + \frac{A_t a_t}{h_t^2}) \theta C^3 \right] \dot{\theta}$$

$$= k_\theta \theta + c_\theta \dot{\theta} \tag{10}$$

where E, A, and h are elastic modulus, viscosity factor, and thickness of elastomeric material, respectively. The subscripts c and t indicate the compression and tension, respectively, and k_θ and c_θ represent the stiffness and viscous damping of the beam-column connection.

4 EQUATION OF MOTION

Since the length of the connection device is small compared with the length of beam, the mass of the isolation device can be neglected. The damping coefficient of the beam is assumed to be negligible compared to the damping of the dissipating device. Therefore, the damping coefficient of the connection device is the only damping effect in the structure. Because the connection device is designed and placed to resist the joint rotation only, the viscous damping matrix is a diagonal matrix with the entries at the position corresponding to the joint rotation. The stiffness matrix includes the contributions of beams, columns and dissipative devices. Therefore, the differential equation of motion can be written in matrix form as

$$[M_B]\{\ddot{u}(t)\}+[C_\theta]\{\dot{u}(t)\}+([K_B]+[K_\theta])\{u(t)\}$$

$$= - [M_B]\{\ddot{u}_g\} \tag{11}$$

where $\{\ddot{u}_g(t)\}$ is the seismic horizontal acceleration vector, $[M_B]$, $[K_B]$ are the mass and stiffness matrices derived from beam and column elements, and $[C_\theta]$, $[K_\theta]$ are the viscous damping and stiffness matrices derived from the isolation connection.

5 NUMERICAL APPLICATION

The effectiveness of this new isolation connection is examined by comparing the responses to dynamic time history of framed structures with isolation devices with identical framed structures without isolation devices. The method described in the preceding section is implemented in the analysis of two framed structures, (1) one-bay, six-story frame, and (2) one-bay, ten-story frame. The framed structures are illustrated in Fig. 4. The properties and dimensions of these two frames are tabulated in Tables 1 and 2. The fundamental periods for the six-story rigidly connected frame is 0.85 second, and for the ten-story rigidly connected frame is 1.22 second. The durometer of the elastomeric material of the isolation devices used for these two examples is 90. The thickness of the elastomeric pads of the isolation devices is 9/16 inch for the bottom pad and 9/32 inch for the top pad. The frames were analyzed using time step by step integration schemes. In the analysis of the rigidly connected structures, linear elastic behavior with zero viscosity damping was assumed.

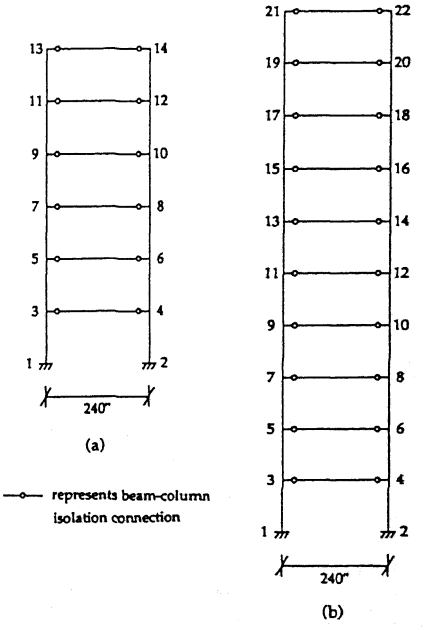

Fig. 4. Frame structures (a) six-story (b) ten-story.

Table 1. Properties of six-story frame

Story	Column	Beam	Mass (K-sec^2/in)
1	W14X74	W24X76	0.1128
2	W14X74	W24X76	0.1128
3	W14X48	W21X57	0.1128
4	W14X48	W21X57	0.1128
5	W14X30	W14X82	0.1128
6	W14X30	W14X82	0.096

Table 2. Properties of ten-story frame

Story	Column	Beam	Mass (K-sec^2/in)
1	W14X257	W21X132	0.108
2	W14X257	W21X132	0.108
3	W14X211	W21X132	0.108
4	W14X211	W21X132	0.108
5	W14X176	W21X132	0.108
6	W14X176	W16X100	0.108
7	W14X132	W16X100	0.108
8	W14X132	W16X100	0.108
9	W14X74	W16X100	0.108
10	W14X74	W14X82	0.084

Three different earthquake accelerations were used as input ground motion to carry out the dynamic time history analysis, (a) Whittier Narrow earthquake, (b) El Centro (Imperial Valley) earthquake, and (c) San Fernando (Pacoima Dam) earthquake. The characteristics of these earthquake motions were tabulated in Table 3. The analysis was conducted for a duration of the first 20 seconds of each earthquake record which includes the most severe motion of each. The earthquake motion was assumed to act horizontally. The unisolated structure was assumed to remain linear elastic, with zero viscosity damping. The analysis was performed using Newmark-β method (γ=1/2, β=1/4) with time step 1/2000 second. Because of the nonlinearity of the isolation connections, the viscosity damping matrices need to be updated at the end of each time step by using eqs. 4 and 5.

Table 3. Earthquake motion used in this study

Notation	Record	Peak Accel. (g)	Predominate frequency range (Hz)	Richter Scale
Whittier Narrow (360°)	East Los Angeles, 10/1/1987	0.45	4-7	6.1
El Centro (S00E)	Imperial Valley 5/18/1940	0.34	1-4	6.7
San Fernando (S74W)	San Fernando, Pacoima Dam, 2/9/1972	1.08	0.25-2	6.4

The effectiveness of the proposed structural model was studied by comparing the analytical response of the frame equipped with the energy dissipating devices to the response of the frame with regular rigid connections. The lateral displacements of the top floor of the six-story frame are compared in Figs. 5 through 7. The lateral displacements of top floor of the ten-story frame are compared in Figs. 8 through 10.

6 CONCLUSIONS AND DISCUSSIONS

The comparison of the responses of the framed structures studied in this work indicate that the lateral displacements of the unbraced frames are reduced significantly by energy dissipating isolation connections. It is apparent that the lateral displacements of the structures with isolation are reduced by about 30 percent of those without isolation. In addition, the response period is increased significantly.

In this study, the isolation devices for frames were found to be more efficient in improving the dynamic response when the structures were subjected to Whittier Narrow earthquake and San Fernando earth

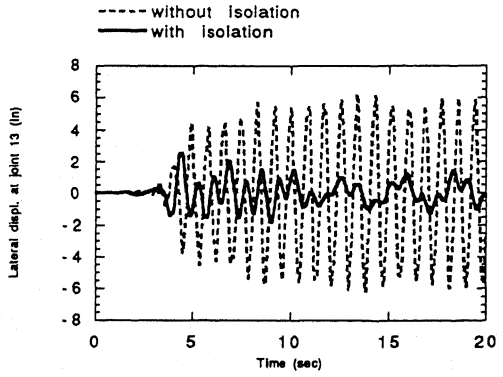

Fig. 5. Lateral displacement at top floor of the six-story frame for Whittier Narrow earthquake.

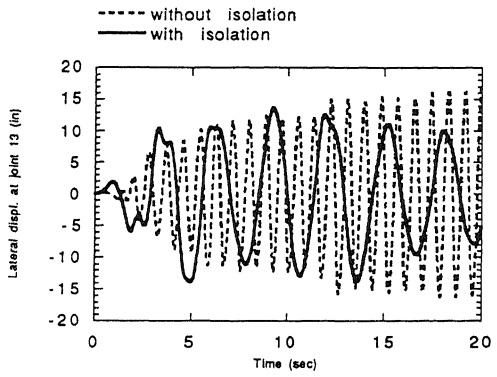

Fig. 6. Lateral displacement at top floor of the six-story frame for EL Centro earthquake.

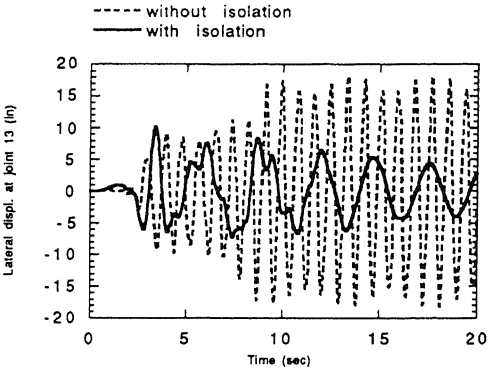

Fig. 7. Lateral displacement at top floor of the six-story frame for San Fernando earthquake.

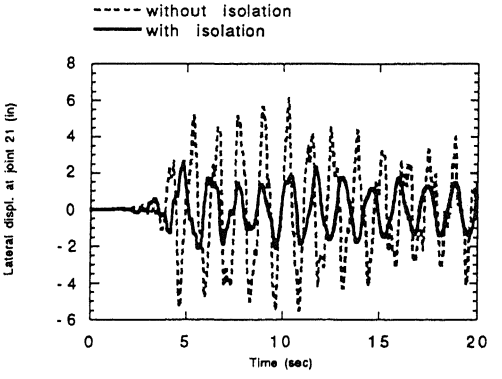

Fig. 8. Lateral displacement at top floor of the ten-story frame for Whittier Narrow earthquake.

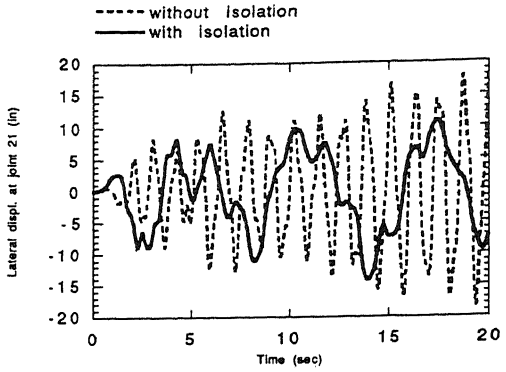

Fig. 9. Lateral displacement at top floor of the ten-story frame for EL Centro earthquake.

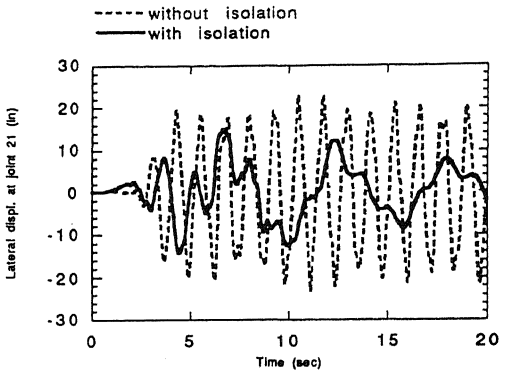

Fig. 10. Lateral displacement at top floor of the ten-story frame for San Fernando earthquake.

quake than when they were subjected to El Centro earthquake. This may be due to the fact that the El Centro earthquake had a longer duration of strong motion. It is known that a ground motion with a moderate peak acceleration and long duration may cause more damage than a ground motion with a large acceleration and a short duration.

It is known that peak acceleration primarily influences the vibration amplitude. For San Fernando earthquake which had 1.08g peak acceleration, the maximum displacements were higher than those in the other two earthquakes. For high-rise unbraced framed structures, the excessive displacement can cause large deformation of the elastomeric pads. Therefore, thicker elastomeric pads should be considered for high peak acceleration earthquake input.

It is known that the characteristics of an earthquake such as peak ground motion, duration of strong motion, and frequency content have an effect on the response. Therefore, a particular frame will always exhibit different levels of performance in different earthquakes. However, the three severe and well-known earthquake records that have been used in this study

cover a wide range of excitation frequencies, duration of strong motion and peak ground motion. Thus, the conclusions regarding to the performance of the isolation system studied in this work, have validity within these limits.

REFERENCES

Ahmadi, G., Papageorgiou, A. S., Tadjbaksh, I. G., and Lin, B. C. 1990. Performance of Earthquake Isolation System. *J. of Struc. Div.*, ASCE, 116(2): 446-461

Bergman, D. M. and Hanson, R. D. 1986. Characteristics of Viscoelastic Mechanic Damping Devices. *Proc. of a Seminar and Workshop on Base Isolation and Passive Energy Dissipation*, Mar. 12-14, San Francisco, CA: 231-240.

Gasparini, D. A., Curry, L. W., and DebChaudbury, A. 1980. Damping of Frames with Viscoelastic Infill Panels. *J. Struct. Div.*, ASCE, 107(5): 889-905.

Gasparini, D. A., DebChaudbury, A., and Curry, L. W. 1981. Damping of Frames with Constrained Viscoelastic Layers. *J. Struct. Div.*, ASCE, 106(1): 115-131.

Hsu, S. Y. and Fafitis, A. 1990. Dynamic Modeling of Energy Dissipating Viscosity Isolators for Structure. *International Conference. Strueng and Femcad*, Nov 6-8, Los Angeles, CA: 399-411.

Hsu, S. Y. and Fafitis, A. 1992a. Dynamic Response of Framed Structures with Energy Dissipating Viscoelastic Connections. *ASME 1992 Workshop on Advanced Dynamics*, Houston, Texas, Jan. 1992.

Hsu, S. Y. and Fafitis, A. 1992b. Seismic Analysis and Design of Frames with Viscoelastic Connections. *J of Struc.*, ASCE. (To appear 1992).

Kelly, J. M. 1982. Aseismic Base Isolation. *Shock Vib. Dig.* 14, No. 5: 17-25.

Kelly, J. M. and Koh, C. G. 1990. Application of Fractional Derivatives to Seismic Analysis of Base Isolated Models. *Earthquake Engrg. and Struc. Dyn.*, Vol. 19: 229-241.

Lin, R. C., Liang, L., Soong, T. T., Zhang, R. H., and Mahmoodi, P. 1991. An Experimental Study on Aseismic Behavior of Viscoelastically Damped Structures. *Engrg. Struct.*, Vol. 13: 75-84.

Liu, E. M. and Chen, W-F. 1986. Analysis and Behavior of Flexibly-Jointed Frames. *Engrg. Struct.*, Vol. 8, April: 107-118.

Mahmoodi, P 1969. Structural Dampers. *J. Struct.Div.*, ASCE, 95(8): 1661-1672.

Mahmoodi, P. 1974. Design and Analysis of Viscoelastic Vibration Dampers for Structures. *Proc. INOVA-73 world innovation week conf.*, E.D. Eyrolles, Paris: 25-39.

Mahmoodi, P. and Keel, C. J. 1986. Performance of Structure Dampers for the Columbia Center Building. *in Building Motion in Wind*, ASCE, New York: 83-106.

Mostaghel, N. and Khodaverdian, M. 1987. Dynamic of Resilient-friction Base Isolator (R-FBI). *Earthquake Engrg. and Struc. Dyn.*, 15(3): 379-390.

Newmark, N. M. 1959. A Method of Computation for Structural Dynamics. *J. of Eng. Mech. Div.*, ASCE, Vol. 85, No. EM3: 67-94.

Zhang, R. H., Soong, T. T., and Mahmoodi, P. 1989. Seismic Response of Steel Frame Structures with add viscoelastic dampers. *Earthquake Engrg. and Struct. Dyn.*, Vol. 18, March: 389-396.